Crystallization Kinetics of Ultra High-Molecular Weight Polyethylene in Liquid Paraffin During Solid–Liquid Thermally Induced Phase Separation Process

Chun-Fang Zhang,[1] Yun-Xiang Bai,[1] Jin Gu,[1] Yu-Ping Sun[1,2]

[1]*School of Chemical and Material Engineering, Jiangnan University, Wuxi 214122, China*
[2]*Wuxi Greenpore Membrane Tech, Co. Ltd., Jiangsu Province, China*

Received 30 November 2010; accepted 1 March 2011
DOI 10.1002/app.34429
Published online 17 June 2011 in Wiley Online Library (wileyonlinelibrary.com).

ABSTRACT: The crystallization behaviors of ultra high-molecular weight polyethylene (UHMWPE) in liquid paraffin under isothermal and nonisothermal conditions were studied by differential scanning calorimetry during the solid–liquid thermally induced phase separation (TIPS) process. For isothermal crystallization, the development of relative crystallinity with the crystallization time is analyzed by the Avrami equation with the exponent $n = 2.7$. The relatively high content of secondary crystallization at higher crystallization temperature can be obtained due to the high mobility of UHMWPE chains. For nonisothermal crystallization studies, the Avrami theory modified by Jeziorny is used, and the result is found that the Avrami exponent n is variable around 5 and decreases slightly as the cooling rate decreases. In addition, the extent of secondary crystallization increases with increasing cooling rate. The calculated activation energies are 881 kJ/mol for isothermal crystallization obtained from the Arrhenius equation and 462 kJ/mol for nonisothermal crystallization from the Kissinger equation, respectively. © 2011 Wiley Periodicals, Inc. J Appl Polym Sci 122: 2442–2448, 2011

Key words: ultra high-molecular weight polyethylene; isothermal crystallization; nonisothermal crystallization; kinetics; Avrami analysis

INTRODUCTION

Thermally induced phase separation (TIPS) is one of the main techniques for the preparation of polymeric porous membranes by controlling phase separation.[1,2] In its simplest form, a polymer is dissolved in a high-boiling, low-molecular weight diluent to form a homogeneous solution at the high temperature. Then, the solution is cast or extruded into the desired shape followed by a cooling process to induce phase separation. Finally, the diluent is removed from the polymer/diluent systems to yield a microporous structure.[3] According to the mechanism of phase separation, TIPS can be classified into two processes: liquid–liquid (L–L) phase separation and solid-liquid (S–L) phase separation.[4,5] As for L–L phase separation, droplets of diluent rich phase form within a continuous matrix of polymer rich phase. The size of droplets is closely related to the pore size of membrane. For S–L phase separation, the polymer crystallizes before L–L phase separation. Therefore, the membrane structure is only determined by the polymer crystal behaviors.

The kinetics of droplet growth in L–L phase separation has been widely investigated. McGuire et al.[6,7] simulated the coarsening process for droplets, and the results showed that the theoretically obtained droplets growth rate agree well with the experimental data. However, little works have focused on the crystallization behaviors of polymer in S–L phase separation. Gu et al.[8] studied the crystallization behavior of poly(vinylidene fluoride) (PVDF) in dimethylphthalate, but they focused on the PVDF crystallization in polymer rich phase for L–L phase separation process. Ji et al.[9] investigated the nonisothermal crystallization kinetics of PVDF in dibutyl phthalate/di(2-ethylhexyl)phthalate blends via S–L phase separation through differential scanning calorimetry measurements.

Ultra high-molecular weight polyethylene (UHMWPE) is an attractive material due to its unique unmatchable physical and mechanical properties. Very high molecular weight (typically in the range of 2×10^6 to 16×10^6 Da) and long relaxation time of UHMWPE chains provide a structural foundation for superior toughness and resistance to impact and wear.[10] Li et al.[11] have prepared the porous flat UHMWPE membranes with mineral oil as a diluent and poly(ethylene glycol) (PEG) as an additive via S–L phase separation. They studied the

Correspondence to: Y.-X. Bai (baisir223@163.com).
Contract grant sponsor: National Basic Research Program of China; contract grant number: 2003CB615705.
Contract grant sponsor: Youth Fundation of Jiangnan University; contract grant number: 2009LQN12.

effect of PEG content on the crystallization behavior of UHMWPE and found that the addition of PEG could be beneficial to the improvement of the crystallization rate and crystallinity, but the over addition of PEG went against crystal growth. However, the kinetics parameters of crystallization, such as crystallization rate constant and crystallization activation energy, were not discussed.

In the present study, the isothermal and nonisothermal crystallization kinetics of UHMWPE in LP during S–L phase separation were investigated. Through differential scanning calorimeter measurements, the effects of crystallization temperature and cooling rate on the Avrami parameters and crystallization rate constant are discussed. Furthermore, the crystallization activation energies of UHMWPE in LP for isothermal and nonisothermal crystallization process are also calculated using the Arrhenius and Kissinger equation, respectively.

EXPERIMENTAL

Materials

UHMWPE ($M_n = 1.5 \times 10^6$) was kindly supplied by Beijing No.2 Auxiliary Agent Factory, Beijing, China. Liquid paraffin (bp $>$ 300°C, density is 0.864–0.860 g/mL at 20°C) was supplied by Hangzhou Chemical Reagent Co., China.

Preparation of UHMWPE/LP blends samples

Homogeneous sample of ultra high-molecular weight polyethylene (UHMWPE)/LP blend with 10 wt % UHMWPE content was prepared in the mixing chamber of a rheometer (HAAKE HBI System 90). The mixing condition was melting temperature, 170°C; rolling speed, 64 r/min; and mixing time, 10 min. Then, the blends were cooled at room temperature for crystallization kinetic tests.

Isothermal and nonisothermal crystallization process

For isothermal crystallization kinetic studies, the UHMWPE/LP blend samples were first heated to 200°C, maintained for 5 min to erase thermal history, and then quenched at 100°C/min to the designated crystallization temperatures. The exothermic curves, as a function of time, were then recorded.

To reveal the nonisothermal crystallization kinetics, the UHMWPE/LP sample was first heated to 200°C and maintained for 5 min to erase thermal history, and then the sample was cooled to 30°C at a cooling rate of 2, 4, 8, and 30°C/min, respectively. The exothermic curves of heat flow with the decrease of temperature were recorded.

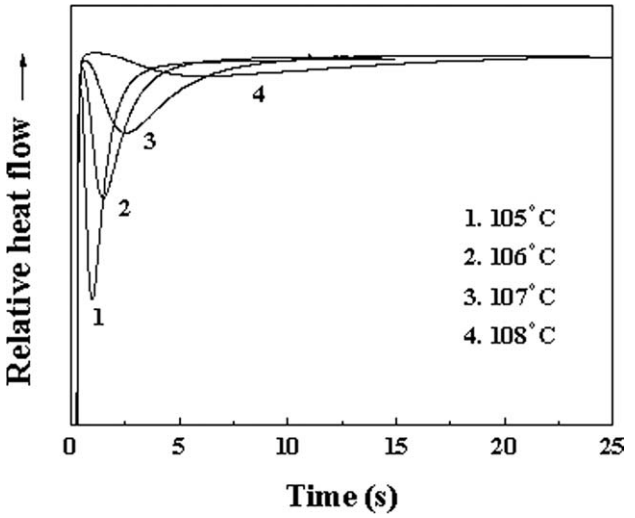

Figure 1 Relative heat flow of isothermal crystallization of UHMWPE/LP blend at different crystallization temperatures (T_c), UHMWPE content is 10 wt %.

RESULTS AND DISCUSSION

Isothermal crystallization kinetics

Figure 1 shows the isothermal crystallization thermograms of the UHMWPE/LP blend at different crystallization temperature (T_c). It can be seen that the crystallization exothermic peak becomes flatter and the time to reach the maximum degree of crystallization increases as T_c increases, that is, the crystallization rate decreases with the increase of T_c.

The isothermal crystallization kinetics of a material can be analyzed by evaluating the variation of its crystallinity as a function of time at a constant temperature. The relative crystallinity, X_t, at different crystallization time can be defined according to the equation as following:

$$X_t = \frac{\int_0^t (dH_c/dt)dt}{\int_0^\infty (dH_c/dt)dt} = \frac{\Delta H_t}{\Delta H_\infty} \quad (1)$$

where dH_c/dt is the rate of crystallization heat evolution, ΔH_t is the heat generated at time t, and ΔH_∞ is the total heat generated up to the end of the crystallization process. The X_t of 10 wt % UHMWPE/LP blend at different T_c was plotted in Figure 2. It can be seen that all the curves have the similar "S" shape. Furthermore, characteristic sigmoid isotherms shift to the right with the increase of T_c, which means the crystallization rate of UHMWPE becomes slower at a higher T_c.

Development of relative crystallinity can be analyzed using the Avrami equation.[12]

$$X_t = 1 - \exp(-Kt^n) \quad (2)$$

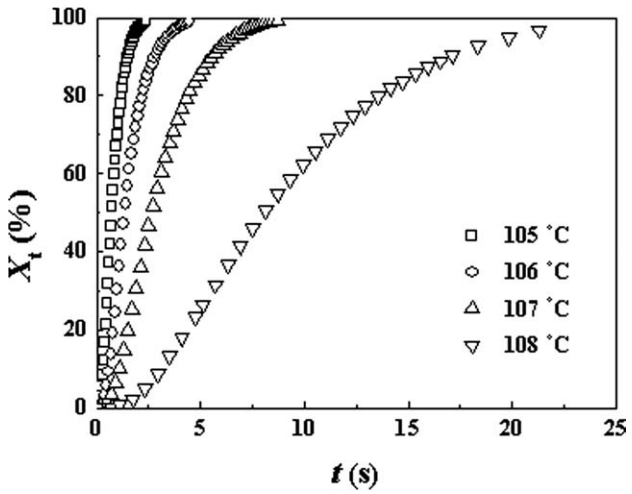

Figure 2 Development of relative crystallinity, X_t, with crystallization time, t, for UHMWPE/LP blend at different crystallization temperatures during isothermal crystallization, UHMWPE content is 10 wt %.

or

$$\log[-\ln(1 - X_t)] = n \log\ t + \log\ K \tag{3}$$

where n is a constant, which is determined by the mechanism of nucleation and the formation of crystal growth. K is crystallization rate constant concerning the nucleation and the growth processes. From a graphic representation of $\log[-\ln(1 - X_t)]$ versus $\log t$, the Avrami exponent n (slope of the straight line) and the crystallization rate constant K (intersection with the y-axis) can be obtained.

Figure 3 illustrated the plot of $\log[-\ln(1 - X_t)]$ versus $\log t$ at the different crystallization temperatures for a UHMWPE/LP blend with a UHMWPE content of 10 wt %. It can be seen that each curve for the isothermal crystallization of UHMWPE/LP blend shows an initial linear portion and then subsequently tends to level off. This deviation compartmentalizes the whole crystallization process into two stages, a primary and secondary crystallization process. The primary crystallization process consists of the radial growth of the crystallites until impingement, and the secondary crystallization process involves the growth or subsidiary lamellae or lamella thickening within the crystallites in the later stage of isothermal crystallization process.[13] Therefore, secondary crystallization as a source of structural evolution is closely relative to the mechanical strength of membrane. The percentage of secondary crystallization in total crystallinity, X_s, can be defined according to the equation as following:

$$X_S = 1 - X_P \tag{4}$$

where X_p is the relative crystallinity at the end of the primary process. Figure 4 illustrates the variation of X_s with isothermal crystallization temperature for UHMWPE/LP blend with a UHMWPE content of 10 wt %. It can be seen that the extent of secondary crystallization for the isothermal crystallization at 105°C is relatively small (about 46%). However, it increases dramatically with the enhancement of T_c and reaches 78% at 108°C. The relatively high content of secondary crystallization at higher T_c can be attributed to the higher mobility of UHMWPE chains. As we know that the diffusion of UHMWPE chains toward the crystallization growth front will become easy and frequent with the increase of T_c. Therefore, a great part of crystallizable chains, which did not incorporate into crystallites at primary crystallization, is more prone to crystallize into thinner less-perfect lamellar during secondary crystallization

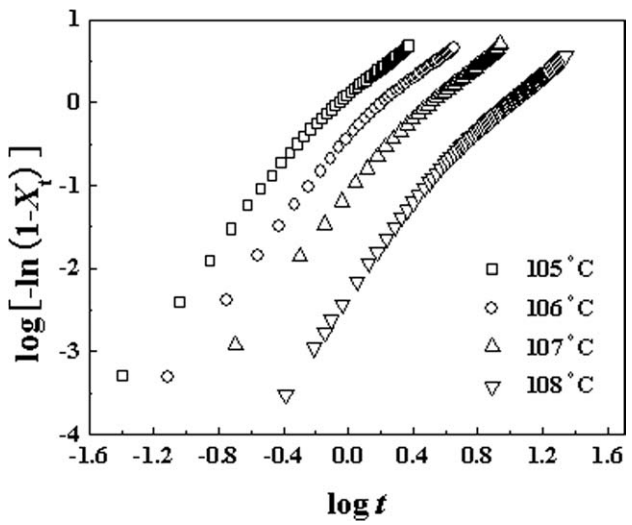

Figure 3 Avrami curves for 10 wt % UHMWPE in liquid paraffin at different crystallization temperatures.

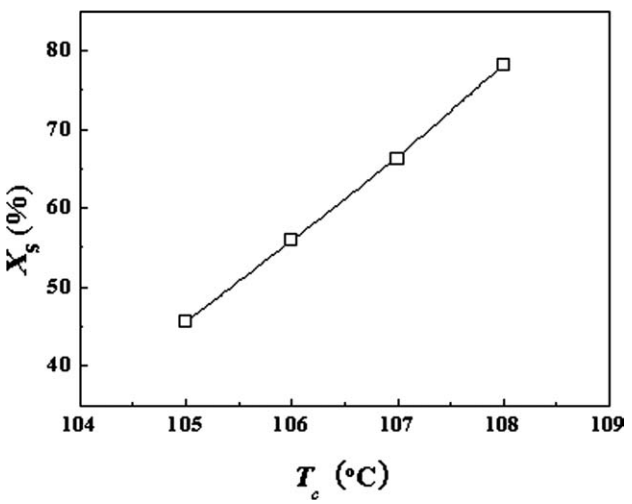

Figure 4 Plot of the proportion of secondary crystallization (X_s) versus T_c for the isothermal crystallization of UHMWPE/LP blend, UHMWPE content is 10 wt %.

TABLE I
Parameters of Isothermal Crystallization of 10 wt % UHMWPE/LP Blend

T_c (°C)	K (s^{-1})	n
105	2.42	2.66
106	4.31×10^{-1}	2.66
107	8.38×10^{-2}	2.62
108	4.68×10^{-3}	2.81

and leads to the enhancement of the secondary crystallization content accordingly.

Fitting the initial linear portion of $\log[-\ln(1 - X_t)]$ versus $\log t$ allows us to determine n and K in primary crystallization stage, and the values are listed in Table I. A narrow spread of n values centered at 2.7 can be obtained. Generally, an n with value close to 3 is attributed to three-dimensional crystal growth (spherical structure) resulting from instantaneous athermal nucleation process. On the other hand, an n value between two and three represents non-three-dimensional-truncated spherical structures resulting from instantaneous nucleation, which is controlled by diffusion process. So, the nonintegral n values indicate the presence of the combination of thermal and athermal mixed nucleation mechanisms.[14] In the present case for UHMWPE/LP blend, it can be observed that the exponent n is close to 2.7 when T_c changed at the studied T_c range from 105 to 108°C. This indicates that a two-dimensional and a spherical three-dimensional crystal growth occur simultaneously with a combination of thermal and a thermal nucleation under the studied experimental conditions.

Crystallization half-time, $t_{1/2}$, is defined as the time at which the extent of crystallization is 50%. It can be read conveniently from Figure 2 and is also regarded as a very important crystallization kinetic parameter. Usually, $t_{1/2}$ is used to characterize the crystallization rate directly. The greater the $t_{1/2}$ value, the lower the crystallization rate. Furthermore, $t_{1/2}$ can also be derived from the crystallization rate parameter K according to eq. (5)[15]:

$$t_{1/2} = \left(\frac{\ln 2}{K}\right)^{1/n} \tag{5}$$

Figure 5 shows the dependency of $t_{1/2}$ on T_c for UHMWPE/LP blend with a UHMWPE content of 10 wt %, and the values of $t_{1/2}$ obtained from Figure 2 are also shown in Figure 5. Obviously, the higher the T_c, the larger the $t_{1/2}$, which indicates that the crystallization rate is lower at higher T_c. Meantime, the values of $t_{1/2}$ calculated from eq. (5) are in agreement with those obtained from Figure 2, which suggests that the Avrami analysis works very well in describing the isothermal crystallization process of UHMWPE/LP blend.

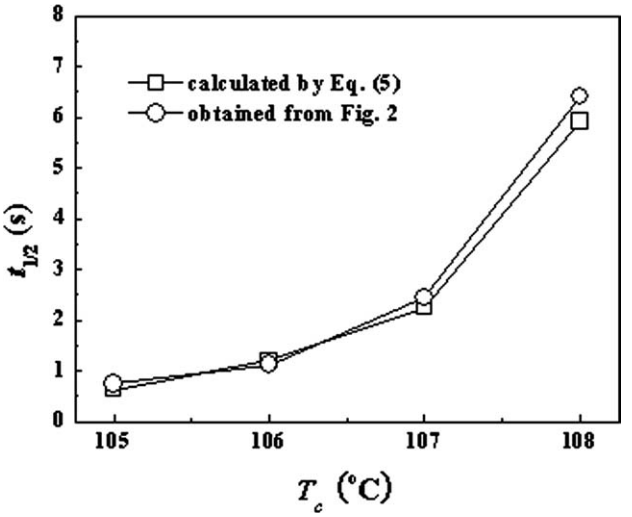

Figure 5 Plot of $t_{1/2}$ versus T_c for the isothermal crystallization of UHMWPE/LP blend, UHMWPE content is 10 wt %.

Obtained from the intercept of the Avrami plot (Fig. 3), the crystallization rate parameter can be used to determine the activation energy for crystallization. Thus, K can be approximately described by an Arrhenius equation as follows:

$$K^{1/n} = K_0 \exp(-\Delta E/RT_c) \tag{6}$$

where K_0 is a temperature-independent pre-exponential factor, ΔE is an activation energy, and R is a gas constant. $\Delta E/R$ is determined by the linear regression of the experimental data of $(1/n)\ln K$ versus $1/T_c$ as plotted in Figure 6, and the crystallization activation energy is calculated as 881 kJ/mol for the isothermal crystallization of 10 wt % UHMWPE/LP blend.

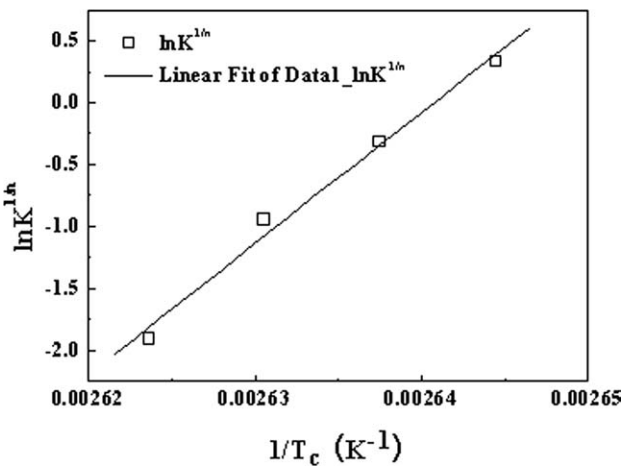

Figure 6 Arrhenius plot of UHMWPE/LP blend during the isothermal crystallization, UHMWPE content is 10 wt %.

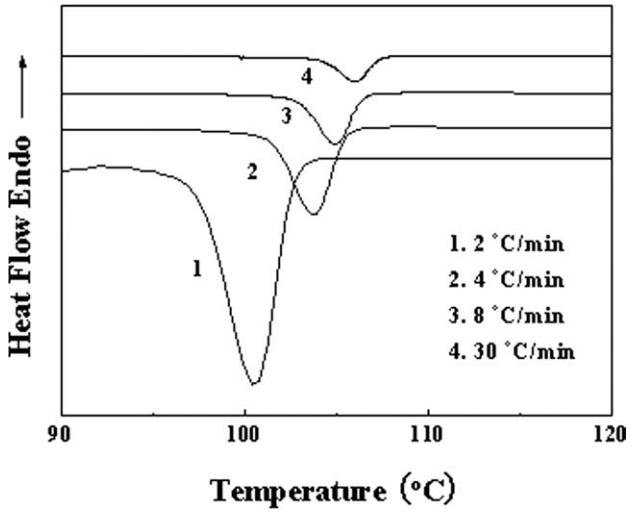

Figure 7 Differential scanning calorimeter curves of nonisothermal crystallization of UHMWPE/LP blend at different cooling rate, UHMWPE content is 10 wt %.

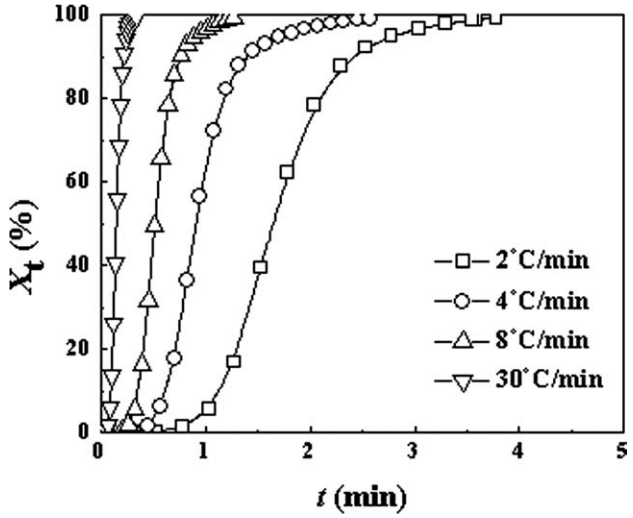

Figure 8 Development of relative crystallinity, X_t, with crystallization time, t, for UHMWPE/LP blend during nonisothermal crystallization, UHMWPE content is 10 wt %.

Nonisothermal crystallization kinetics

The nonisothermal crystallization of UHMWPE/LP blend was investigated at different cooling rates. The exothermal curves of heat flow developing with temperature were recorded as shown in Figure 7. It is notable from Figure 7 that the T_c shifts to a lower temperature with the increase of cooling rate. This observation is typical and common for most semicrystalline polymer while crystallizing nonisothermally and can be explained that a lower cooling rate provides a relatively long time to promote sufficient movement of polymer segments for the growth of crystallization when the polymer is undergoing a crystallization process. When cooled at a relatively rapid rate, however, polymer segments are prone to be frozen before the formation of regular crystallite, thus decreasing the crystallization temperature.

Integration of the exothermal peaks in Figure 7 can give the variation of relative crystallinity as a function of time, and the results are shown in Figure 8. The relationship between T_c and the nonisothermal crystallization time, t, can be determined by eq. (6).

$$t = \frac{T_0 - T}{\Phi} \tag{7}$$

where T is the crystallization temperature during the nonisothermal crystallization process, T_0 is the initial temperature at the beginning of crystallization ($t = 0$), and Φ is the cooling rate. It can be seen from Figure 8 that the higher the cooling rate, the shorter the crystallization time. Generally, increasing the cooling rate can provide the system with more energy to improve the activity of chain segment, thus result in the increasing of crystallization rate.

Just like isothermal process, nonisothermal crystallization can also be analyzed by the Avrami equation. But considering the nonisothermal characterization of the process investigated and the effect of the cooling rate, Jeziorny[16] modified the Avrami equation with the cooling rate as follows:

$$\log[-\ln(1 - X(t))] = n \log\ t + \Phi \log\ Z_c \tag{8}$$

where Z_c is the kinetic crystallization rate constant. Figure 9 shows the plots of $\log[-\ln(1 - X(t))]$ versus $\log\ t$ for UHMWPE/LP blends at different cooling rate.

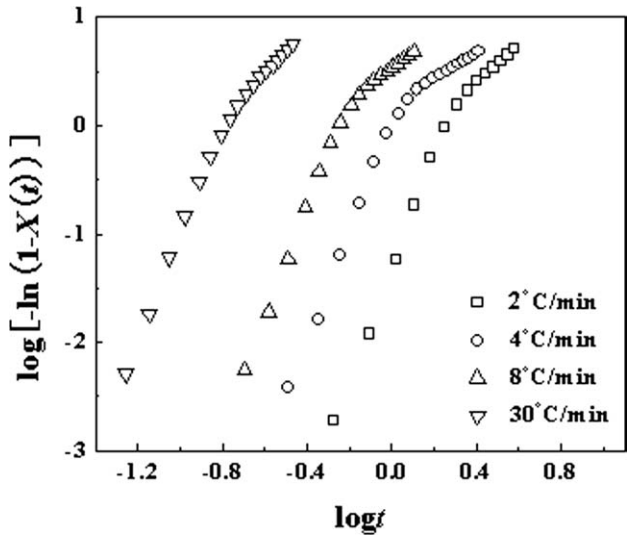

Figure 9 Plots of $\log[-\ln(1 - X(t))]$ versus $\log\ t$ for UHMWPE/LP blend during nonisothermal crystallization, UHMWPE content is 10 wt %.

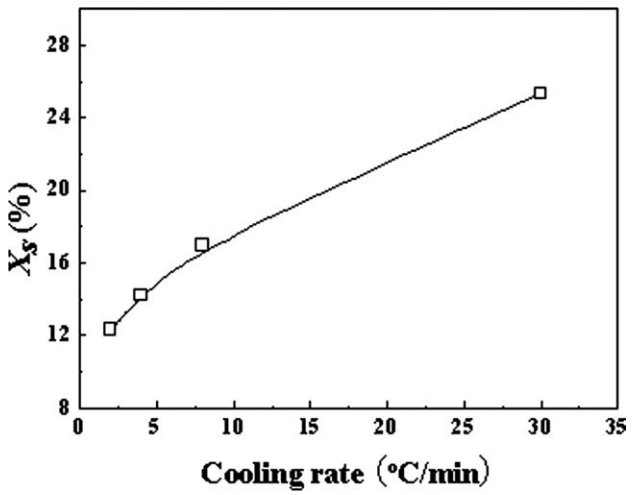

Figure 10 Variations of X_S with cooling rate of UHMWPE/LP blend for nonisothermal crystallization, UHMWPE content is 10 wt %.

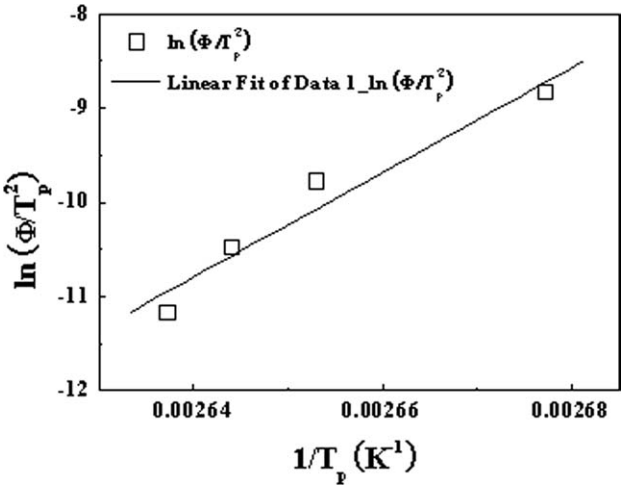

Figure 11 Kissinger plots of the nonisothermal crystallization for UHMWPE/LP blend, UHMWPE content is 10 wt %.

Similar to the Avrami curve of the isothermal crystallization, all plots of $\log[-\ln(1 - X(t))]$ versus $\log t$ show the obvious roll-off at the later stage of crystallization, which indicates that the secondary crystallization of UHMWPE occurs under nonisothermal crystallization conditions. The X_s for nonisothermal crystallization can also be determined according to eq. (4). Figure 10 illustrates the dependence of X_s on the cooling rate under the nonisothermal crystallization conditions. It can be seen that the value of X_s increases with the increase of the cooling rate. In common, the secondary crystallization was considered to be the further perfection of crystal, which was caused by the reorganization of initially poorly crystallized macromolecules or small and metastable crystals. At higher cooling rate, UHMWPE chains have little time to move to the crystallization growth front to form the perfect crystal. Thus, most of the imperfect or metastable crystals would be developed into the perfect ones through the reorganization of molecular chains at the secondary crystallization stage, which resulted in the higher content of the secondary crystallization accordingly.

Fitting the initial linear portion of primary crystallization stage in Figure 9, the values of n and Z_t can be obtained for UHMWPE/LP blend under nonisothermal crystallization conditions and listed in Table II. The Avrami exponent n is variable around 5 as the cooling rate changed. Generally, the reported values of n for PE range from 2 to 4 (mostly for isothermal crystallization).[17–19] High values of n for UHMWPE/LP blends may be caused by high viscosity, which would lead to a more complicated crystallization mechanism. It is also found from Table II that n decreases slightly as the cooling rate decreases. This result is in consistent with Eder[20] and Zou's work.[21] This is because that the fast crystallization rate of UHMWPE at higher cooling rate would prevent the spherulites from their full development and result in the decrease of the value of n. The data in Table II also shows that the values of Z_c [calculated from eq. (4)] for UHMWPE/LP blend increases as the increase of cooling rate. The enhancement of Z_c means an increase of crystallization rate, which is in consistent with our results above.

Considering the influence of the various cooling rates Φ on the nonisothermal crystallization process, Kissinger proposed that the activation energy can be determined by calculating the variation of the crystallization peak with the cooling rate.[22] It reads:

$$\frac{d\left(\ln\frac{\Phi}{T_p^2}\right)}{d\left(\frac{1}{T_P}\right)} = -\frac{\Delta E}{R} \tag{9}$$

where R is the gas constant and T_p is the crystallization peak temperature. Graphs of $\ln(\Phi/T_p^2)$ versus $1/T_p$ are shown in Figure 11. The slope of the curve determines $\Delta E/R$. Activation energy ΔE for

TABLE II
Kinetic Parameters of Nonisothermal Crystallization for UHMWPE/LP Blend

Φ (°C/min)	T_p (°C)	n	Z_c
2	106.02	5.14	0.229
4	105.04	5.06	1.039
8	103.78	5.02	1.448
30	100.35	4.97	1.361

nonisothermal crystallization is found to be 462 kJ/mol, which is smaller than that of the isothermal crystallization process.

CONCLUSIONS

The investigation of the isothermal and nonisothermal crystallization kinetics of UHMWPE/LP blend was carried out through differential scanning calorimetry during S–L TIPS process. The Avrami equation was used to analyze the isothermal crystallization of UHMWPE. From the narrow spread of n values centered at 2.6, it was proposed that the isothermal crystallization may proceed via two-dimensional and a spherical three-dimensional growth simultaneously. This can be attributed to that a high mobility of UHMWPE chains at higher T_c resulted in the relatively high content of secondary crystallization. Then, the activation energy 881 kJ/mol was obtained by crystallization rate parameter, K, at different crystallization temperatures according to the Avrami equation. Furthermore, the Avrami theory modified by Jeziorny was used to analyze the nonisothermal crystallization of UHMWPE in LP. The results showed that the Avrami exponent n is variable around 5 and decreases slightly as the cooling rate decreases, while the extent of secondary crystallization increases with increasing the cooling rate. The activation energy obtained according to the Kissinger method was lower than that of the isothermal crystallization process.

References

1. Fu, X.; Matsuyamaa, H.; Teramoto, M.; Nagai, H. Sep Purif Technol 2005, 45, 200.
2. Gu, M. H.; Zhang, J.; Wang, X. L.; Tao, H. J.; Ge, L. T. Desalination 2006, 192, 160.
3. Hiatt, W. C.; Vitzthum, G. H.; Wagener, K. B.; Gerlach, K.; Josefiak, C. ACS Symp Ser 1985, 269, 229.
4. Lloyd, D. R. J Membr Sci 1990, 52, 239.
5. Lloyd, D. R.; Kim, S.; Kinzer, K. E. J Membr Sci 1991, 64, 1.
6. McGuire, K. S.; Laxminarayan, A.; Martula, D. S.; Lloyd, D. R. J Colloid Interface Sci 1996, 182, 46.
7. McGuire, K. S.; Laxminarayan, A.; Lloyd, D. R. Polymer 1995, 36, 4951.
8. Gu, M. H.; Zhang, J.; Wang, X. L.; Ma, W. Z. J Appl Polym Sci 2006, 102, 3714.
9. Ji, G. L.; Zhu, B. K.; Zhang, C. F.; Xu, Y. Y. J Appl Polym Sci 2008, 107, 2109.
10. Turell, M. B.; Bellare, A. Biomaterials 2004, 25, 3389.
11. Li, N.; Xiao, C.; Zhang, Z. J Appl Polym Sci 2010, 117, 720.
12. Avami, M. J Chem Phys 1939, 7, 1103.
13. Jenkins, M. J.; Harrison, K. L. Polym Adv Technol 2006, 17, 474.
14. Janeschitz-Kriegl, H.; Ratajski, E.; Wippel, H. Colloid Polym Sci 1999, 277, 217.
15. Li, J.; Zhou, C. X.; Wang, G.; Tao, Y.; Liu, Q.; Li, Y. Polym Test 2002, 21, 583.
16. Jeziorny, A. Polymer 1978, 19, 1142.
17. Hay, J. N.; Perzekop, Z. J. J Polym Sci Part B: Polym Phys 1978, 16, 81.
18. Gupta, A. K.; Rana, S. K.; Deopura, B. L. J Appl Polym Sci 1994, 51, 231.
19. Hay, J. N.; Mills, P. J. Polymer 1982, 23, 1380.
20. Eder, M.; Wlochowicz, A. Polymer 1983, 24, 1593.
21. Zou, P.; Tang, S. W.; Fu, Z. Z.; Xiong, H. G. Int J Therm Sci 2009, 48, 837.
22. Kissinger, H. E. J Res Nat Stand 1956, 57, 217.